Available online at www.sciencedirect.com
SCIENCE DIRECT®
Journal of Sound and Vibration 278 (2004) 365–381
JOURNAL OF SOUND AND VIBRATION
www.elsevier.com/locate/jsvi

Periodic monitoring of physical property changes in a concrete box-girder bridge

Sanghyun Choi[a], Sooyong Park[b,*], Robert Bolton[c], Norris Stubbs[d], Charles Sikorsky[e]

[a] *Structural Systems & Site Evaluation Department, Korea Institute of Nuclear Safety, Daejeon 305-600, South Korea*
[b] *School of Architecture, Youngsan University, Junam-ri, Ungsang-up, Yangsan-si, Kyongnam 626-847, South Korea*
[c] *Department of Engineering Technology and Industrial Distribution, Texas A&M University, College Station, TX 77843, USA*
[d] *Department of Civil Engineering, Texas A&M University, College Station, TX 77843, USA*
[e] *State of California Department of Transportation, Office of Earthquake Engineering, Sacramento, CA 94274, USA*

Received 2 December 2002; accepted 7 October 2003

Abstract

The objective of this paper is to quantitatively evaluate the rate of possible structural property changes of a reinforced concrete box girder bridge over a 2-year period using a system identification technique. The structural condition of the concrete box-girder bridge is monitored four times from December 1997 to October 1999 and the physical property changes are estimated using the frequency-based system identification technique. Modal parameters (resonant frequencies and modal amplitudes) for the bridge are extracted from the measured frequency response functions. The validation of the system identification scheme is demonstrated through a numerical study using the finite element model of the same bridge structure.

1. Introduction

In recent years, with the advent of better sensing technology and non-destructive damage detection technique, researchers have focused more attention on developing practical and robust structural health monitoring systems [1,2]. Knowledge of the structural integrity of a system in real time is a critical issue, since the event of failure could be catastrophic. Following the

*Corresponding author. Tel.: +82-55-380-9495; fax: +82-42-868-0523.
E-mail addresses: schoi@kins.re.kr (S. Choi), sypark@ysu.ac.kr (S. Park), bbolton@tamu.edu (R. Bolton), n-stubbs@tamu.edu (N. Stubbs), charles_sikorsky@dot.ca.gov (C. Sikorsky).

0022-460X/$ - see front matter © 2003 Published by Elsevier Ltd.
doi:10.1016/j.jsv.2003.10.005

occurrence of extreme events, such as strong-motion earthquakes, the safety or reliability of structures such as bridges is a major concern to government officials and bridge engineers. The seriously deteriorating condition of the transportation infrastructure has stimulated great interest in the monitoring of the integrity of bridge systems. In addition, with respect to the maintenance of structural systems, monitoring the structural health condition at regular intervals could have such beneficial consequences as increase in the productivity of operations, reduction of maintenance costs, and prolongment of the useful service life span. Also, periodic health monitoring could help structural and bridge engineers to improve the efficacy and efficiency of maintenance operations, rehabilitation projects, and replacement decisions.

In response to these concerns, many techniques in non-destructive damage evaluation (NDE) and the evaluation of structural safety have been developed in recent years. During the past two decades for example, a significant amount of research has been conducted in the area of NDE using the dynamic properties of a structure [3,4]. However, despite an enormous number of techniques and theories [5], most of the proposed methods exhibit one or more of the following shortcomings. First, in many instances, the research efforts have been limited to the analytical studies or controlled laboratory experiments [6,7]. Second, field studies involving periodic health monitoring on an existing structure are almost non-existent in the literature. Third, there are few approaches that attempt to demonstrate over a period of time of the effectiveness of any particular method on a specific structure.

In an attempt to overcome these limitations, the authors have monitored a bridge located in California, the Lavic Road Bridge (Fig. 1), from 1997 as yearly basis [8]. The bridge was suspected of having been constructed with reactive aggregates. The modal tests were performed on the structure in December 1997, September 1998, September 1999, and October 1999, respectively. The resulting modal data were then used to identify and record the changes in stiffness properties of deck, column-footing, and abutment–soil system. A frequency-based system identification (SI) technique that can simultaneously account for gross changes in mass, stiffness, and boundary conditions of a structure is utilized in this paper [9]. A description of the theory supporting the

Fig. 1. View of the Lavic Road Bridge.

method, a numerical demonstration of the accuracy and efficiency of the approach, and the application of the method to an existing structure to corroborate the analytical approach are presented in this paper.

The objective of this paper is to quantitatively evaluate the rate of possible structural property changes of the reinforced concrete box-girder bridge. In order to achieve the stated objective, the following steps were performed: (1) a field modal test was performed on the bridge in December 1997; (2) from measured frequency response functions, modal frequencies, modal damping coefficients, and mode shapes were extracted; (3) a 3-D finite element (FE) model of the structure was developed; (4) using the SI technique, the extracted field modal parameters, and the FE model, effective values of the moduli of the deck and column and the effective stiffness of the abutments were estimated; and (5) the bridge was retested three times and the effective stiffness values were determined, as described in Steps 2–4 above, using measurements in September 1998, September 1999, and October 1999, respectively.

2. Theory of SI scheme

Earlier research utilized frequency reduction as the sole measure of damage in large civil structures. The implicit assumptions were identical environmental conditions and constant mass. In the field, however, resonant frequencies are affected by (1) changes in boundary conditions (e.g., dry soil vs. wet soil, and frozen bearings vs. free bearings), (2) changes in temperature, (3) changes in mass (e.g., due to water absorption), and (4) changes in member stiffness. These complications have discouraged the use of frequency changes as a robust approach to damage detection. The SI theory presented in this paper [9] can overcome these limitations since it can simultaneously account for gross changes in mass, stiffness, and boundary conditions of a structure. The SI methodology can be outlined as follows.

Consider a linear skeletal structure with NE members and N nodes. Suppose k_j^* is the unknown stiffness of the jth member of the structure for which M eigenvalues are known. Also, suppose k_j is a known stiffness of the jth member of a FE model for which the corresponding set of M eigenvalues are known. Then, relative to the FE model, the fractional stiffness change of the jth member of the structure, α_j, and the stiffnesses are related according to the following equation:

$$k_j^* = k_j(1 + \alpha_j). \tag{1}$$

Similarly the fractional mass change of the jth member of the structure, β_j, and the masses are related according to the following equation:

$$m_j^* = m_j(1 + \beta_j). \tag{2}$$

The fractional stiffness change and the fractional mass change of NE members may be obtained using the following approximate linearized equation [10]:

$$\mathbf{Z} = \mathbf{F}\boldsymbol{\alpha} - \mathbf{G}\boldsymbol{\beta}, \tag{3}$$

or

$$\mathbf{Z} = [\mathbf{F} \vdots -\mathbf{G}] \begin{Bmatrix} \boldsymbol{\alpha} \\ \boldsymbol{\beta} \end{Bmatrix}, \tag{4}$$

where α is a $NE \times 1$ matrix containing the fractional changes in stiffness between the FE model and the structure, β is a $NE \times 1$ matrix containing the fractional changes in mass between the FE model and the structure, $\mathbf{Z}$ is a $M \times 1$ matrix containing the fractional changes in eigenvalues between the two systems, $\mathbf{F}$ is a $M \times NE$ stiffness sensitivity matrix relating the fractional changes in stiffnesses to the fractional changes in eigenvalues, and $\mathbf{G}$ is a $M \times NE$ mass sensitivity matrix relating the fractional changes in masses to the fractional changes in eigenvalues.

The $M \times NE$, $\mathbf{F}$ matrix can be determined as follows: first, M eigenvalues are numerically generated from the initial FE model; second, the stiffness of the first member of the FE model is modified by a known amount; third, the corresponding set of M eigenvalues are numerically generated for the modified FE model; fourth, the fractional changes between the M initial eigenvalues and M eigenvalues of the modified structure are computed; fifth, each component of the first column of the $\mathbf{F}$ matrix (i.e., the $M \times 1$, $\mathbf{F}$ matrix) is computed by dividing the fractional changes in each eigenvalue by the magnitude of the modification at member one; and finally, the $M \times NE$, $\mathbf{F}$ matrix is generated by repeating the entire procedures for all NE members. The $M \times NE$, $\mathbf{G}$ matrix can be determined in similar manner.

Using the above rationale as a basis, the following seven-step algorithm is utilized to identify a given structure:

1. For a given target structure (e.g., a post-damage state of the structure), identify sufficient eigenfrequencies (note that this procedure only utilizes frequency information).
2. Select an initial FE model of the structure, utilizing all possible knowledge about the design and construction of the structure.
3. As outlined above, compute the sensitivity matrices of the FE model.
4. As outlined above, compute the fractional changes in eigenvalues between the FE model and the target structure.
5. Solve (4) to estimate fractional changes in mass and stiffness.
6. Update the FE model using the results in Step 5 and (1) and (2).
7. Repeat steps 4–6 until $Z \approx 0$ or $\alpha \approx 0$ which indicates that the effective parameters of the structure have been identified.

3. Description of the structure

The Lavic Road Overcrossing is a standard Caltrans-designed reinforced concrete box-girder, constructed in 1968 over Interstate 40. The bridge is located approximately 64 km east of the town of Barstow. The structure is oriented in a north–south direction. The south span is 37.5 m long while the north span is 36.0 m long (Fig. 2). The superstructure is a 2.1 m deep reinforced concrete triple box girder which includes a 10.4 m wide deck and four 0.2 m wide webs spaced at 2.7 m. Wall and deck thickness is approximately 15.2 cm. The structure is supported at the south end by Abutment #1 and at the north end by Abutment #3. The bridge is rigidly connected approximately

at mid-span to a single pedestal 1.5 m diameter column, Bent #2, which in turn is supported on a spread footing located in the freeway median.

4. Numerical verification of the SI scheme

4.1. Description of the FE model

The validation of the SI scheme is demonstrated through a numerical study using the FE model of the same bridge structure. The FE model of the reinforced concrete box-girder bridge was developed using ABAQUS [11]. A schematic of the FE model for the bridge is shown in Fig. 3. The flanges, webs, and diaphragms of the deck were modelled using 976 plate elements. Bent #2 was modelled using 240 brick elements. Abutment #1 (south end) and Abutment #3 (north end) were modelled in the following manner. Each abutment system was modelled using four vertical axial springs in the Z direction and four horizontal axial springs in the Y direction (see Fig. 3). These springs represent the behavior of abutment and the soil–structure interaction between the abutment and the soil. The dimensions of Bent #2 were taken from the as-built plans and the soil–structure interaction between the footing of the column and the soil was modelled using a total of 105 axial springs (35 in the X direction, 35 in the Y direction, and 35 in the Z direction) (see Fig. 3). In all the FE model contained 5925 degrees of freedom.

4.2. Verification of the SI scheme using numerical data

With the FE model of the bridge, the numerical validation of the SI scheme was performed for three different states of the structure. Table 1 shows the randomly selected variations in stiffness

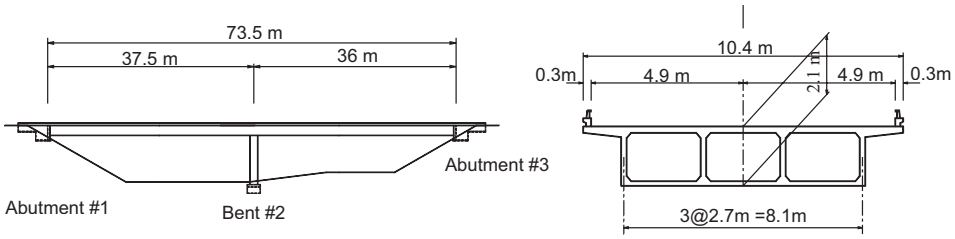

Fig. 2. Layout of the Lavic Road Bridge.

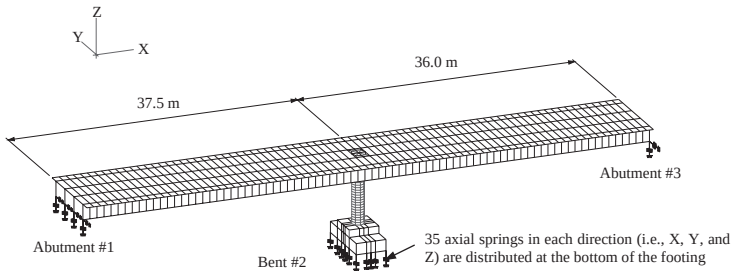

Fig. 3. Schematic of the FE model of the bridge.

and mass parameters. Here, Group 1 includes all elements in the deck; Group 2 includes the column and footing of Bent #2; and Group 3 includes the abutment–soil systems. In Target 1, a 20% increase in mass of Group 1 is assumed. In Target 2, a 20% decrease in mass of Group 1 and a 10% decrease in stiffness of Group 1 are assumed. In Target 3, 20% decrease in mass of Groups 1 and a 10% increase in stiffness of Group 1 are assumed. The identification procedure consisted of the following steps: (1) assume an initial set of parameter values for the FE model, (2) generate stiffness and mass sensitivities using the FE model, and (3) update the material properties of the FE model using the procedure outlined in the preceding section. Initial material properties for the FE model were generated as follows: (1) reinforced concrete was assumed to have a mass density of $\rho = 2400\,\mathrm{kg/m^3}$, Poisson ratio of $v = 0.15$, and the elastic modulus (E) of 20.9 GPa; (2) the soil was assumed to have a modulus of subgrade reaction of $k_s = 342.7\,\mathrm{MN/m}$ (medium dense sand). Note that the spring stiffnesses were obtained from the modulus of subgrade reaction by multiplying by the appropriate area.

The system identification was performed using the first five frequencies. The description of the selected modes as well as the target frequencies is listed in Table 2. With the initial material properties and with the appropriate group stiffness reduced by a known amount, the stiffness sensitivity matrix, **F**, which relates changes in element stiffness to changes in resonant frequencies, was developed. In similar manner, the mass sensitivity matrix, **G**, which relates changes in element mass to changes in resonant frequencies, was developed. The elements of the stiffness sensitivity matrix **F** and the mass sensitivity matrix **G** are listed in Table 3.

The convergence of the system identification scheme is demonstrated in Tables 4–6. From the tables, it can be seen that after three iterations the differences in the corresponding five frequencies of the identified structure and the target structures range from 0.01% to 0.04%. The results of the

Table 1
Initial and target stiffness and mass parameters

Case	Stiffness			Mass
	Group 1 (GPa)	Group 2 (GPa)	Group 3 (MN/m)	Group 1 (kg/m^3)
Initial	20.9	20.9	342.7	2400
Target 1	20.9	20.9	342.7	2880
Target 2	18.8	20.9	342.7	1920
Target 3	23.0	20.9	342.7	1920

Table 2
Resonant frequencies of initial and target structures

Mode	Initial	Target 1	Target 2	Target 3
1 (1st bending in Z dir.)	2.9717	2.7137	3.1744	3.4607
2 (1st bending in Y dir.)	3.1235	2.8551	3.3684	3.5967
3 (2nd bending in Z dir.)	4.3299	3.9543	4.6304	5.0341
4 (1st torsion)	6.4628	5.9153	7.0000	7.3690
5 (2nd bending in Ydir.)	7.5236	6.8681	8.1061	8.6815

Table 3
Mass and stiffness sensitivity matrices using first five modes

Mode	Stiffness			Mass
	Group 1 (GPa)	Group 2 (GPa)	Group 3 (MN/m)	Group 1 (kg/m^3)
1 (1st bending in Z dir.)	0.86929	0.08596	0.05511	−0.90591
2 (1st Bending in Y dir.)	0.67649	0.11620	0.24373	−0.89590
3 (2nd bending in Z dir.)	0.85836	0.04153	0.13075	−0.90512
4 (1st torsion)	0.51284	0.25795	0.26681	−0.88263
5 (2nd bending in Y dir.)	0.69563	0.00239	0.34782	−0.90902

Table 4
System identification for target structure 1

Mode	Frequency of initial FE model	Updated frequencies (Hz)			Frequency of target structure	Error (%)	
		Iter. 1	Iter. 2	Iter. 3		Initial	Final
1	2.9717	2.7324	2.7120	2.7134	2.7137	9.51	0.01
2	3.1235	2.8745	2.8532	2.8548	2.8551	9.40	0.01
3	4.3299	3.9816	3.9517	3.9538	3.9543	9.50	0.01
4	6.4628	5.9542	5.9113	5.9146	5.9153	9.25	0.01
5	7.5236	6.9161	6.8635	6.8672	6.8681	9.54	0.01

Table 5
System identification for target structure 2

Mode	Frequency of initial FE model	Updated frequencies (Hz)			Frequency of target structure	Error (%)	
		Iter. 1	Iter. 2	Iter. 3		Initial	Final
1	2.9717	3.2963	3.1710	3.1737	3.1744	6.39	0.02
2	3.1235	3.5041	3.3658	3.3676	3.3684	7.27	0.02
3	4.3299	4.8092	4.6251	4.6294	4.6304	6.49	0.02
4	6.4628	7.2877	6.9974	6.9984	7.0000	7.67	0.02
5	7.5236	8.4415	8.0985	8.1041	8.1061	7.19	0.02

Table 6
System identification for target structure 3

Mode	Frequency of initial FE model	Updated frequencies (Hz)			Frequency of target structure	Error (%)	
		Iter. 1	Iter. 2	Iter. 3		Initial	Final
1	2.9717	3.8327	3.5086	3.4620	3.4607	14.13	0.04
2	3.1235	3.9585	3.6401	3.5982	3.5967	13.16	0.04
3	4.3299	5.5679	5.0996	5.0362	5.0341	13.99	0.04
4	6.4628	8.0565	7.4561	7.3718	7.3690	12.30	0.04
5	7.5236	9.5860	8.7775	8.6854	8.6815	13.34	0.04

SI for three different target properties are summarized in Table 7. In the table, it is observed that the stiffness and the mass properties of the three target structures are successfully identified.

5. Field modal testing

5.1. Summary of field testing

Four modal tests were performed on the Lavic Road Bridge in December 1997, September 1998, September 1999 and October 1999, respectively. The period between 3rd and 4th field testings spans only 1 month to measure the effect of the Mw 7.1 Hector Mine, California, earthquake. At 9:46 GMT on 16 October 1999, 1 month after the third modal test, the Hector Mine earthquake occurred. The event was located in the Mojave Desert, approximately 76 km east-southeast of Barstow, with epicentral co-ordinates 34.59°N 116.27°W. The Lavic Road Bridge was the only structure in the vicinity to experience major damage from the earthquake. Visual inspection by State of California Department of Transportation personnel within hours of the event indicated major damage to the abutments and the column. The bridge was closed temporarily and temporary shoring was added to the abutments. A view of the south abutment shoring installation is shown in Fig. 4. The visible damage indicated significant north–south horizontal motion occurred during the event. Fig. 5 illustrates the large amount of materials spewed from the south abutment expansion joint. A similar condition was observed at the north abutment. A significant residual subsurface gap was noted between the super structure end-wall diaphragms and roadbed subsoil at both abutments. Figs. 6 and 7 depict views of the shifting and cracking that occurred in the east face abutment wingwalls and superstructure support piers during the event. Residual rotation and transverse shifting of the north–south longitudinal alignment of the bridge was observed after the earthquake. This damage is depicted in Fig. 8. Measurements of the residual centerline horizontal misalignment at the abutments were approximately $+/-100$ mm at both abutment expansion joints. Significant motion was also indicated at the base of the central support column in the roadway median where a 1.0 cm gap was measured between the south face of the column and the surrounding soil. A noticeable increase in surface cracks was also noted near the base of the column. To identify the impact of the seismic event on the bridge, the 4th modal test was performed on 18 October 1999, 2 days after the earthquake.

Table 7
Identified stiffness and mass properties

(Unit)	Initial properties	Target structure 1		Target structure 2		Target structure 3	
		Target	Identified	Target	Identified	Target	Identified
Group 1 (GPa)	20.9	20.9	20.9	18.8	18.9	23.0	23.1
Group 2 (GPa)	20.9	20.9	20.9	20.9	21.0	20.9	20.9
Group 3 (MN/m)	342.7	342.7	342.8	342.7	345.0	342.7	343.8
Mass (kg/m^3)	2400	2880	2885	1920	1933	1920	1925

Fig. 4. A view of temporary shoring installed under the bridge superstructure.

Fig. 5. View of damage to south abutment expansion joint.

The apparatus used in the modal tests consisted of sixteen-channel signal analyzer, tri-axial accelerometers, an impact hammer, and a commercial software package to perform the modal analysis. The accelerometer layout for tests is shown in Fig. 9. The responses of the structure were measured at 30 locations: 26 locations on the deck (E1–E13 and W1–W13) and 4 locations on the column (C1–C4). For all readings, the structure was impacted in the Z direction by an instrumented hammer at the midpoint between accelerometers E3 and E4. Responses in the X, Y, and Z directions were recorded at all locations. A standard modal analysis [12] was performed on the collected data set of transfer functions and modal amplitudes were extracted for each modal frequency. A detailed description of the field testing and the modal analysis are provided in Ref. [13].

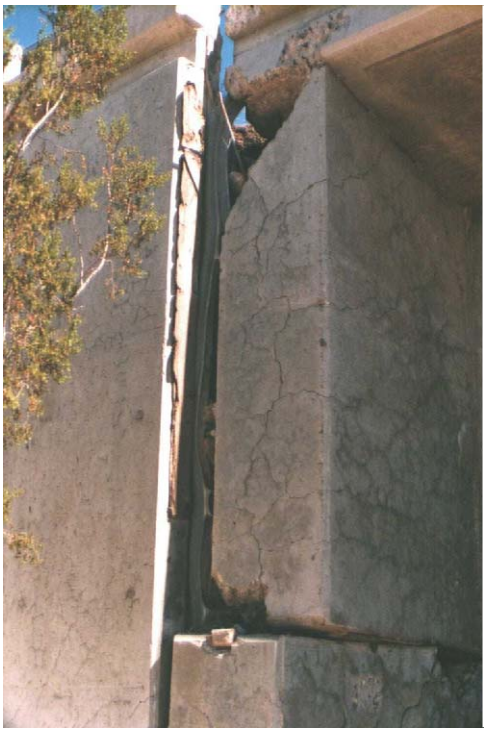

Fig. 6. Damage and misalignment of east wingwall and pier at south bridge abutment.

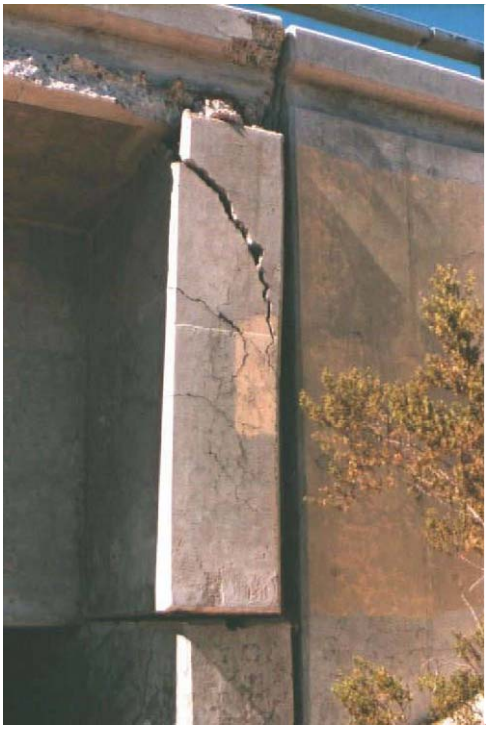

Fig. 7. Damage and misalignment of east wingwall and pier at north bridge abutment.

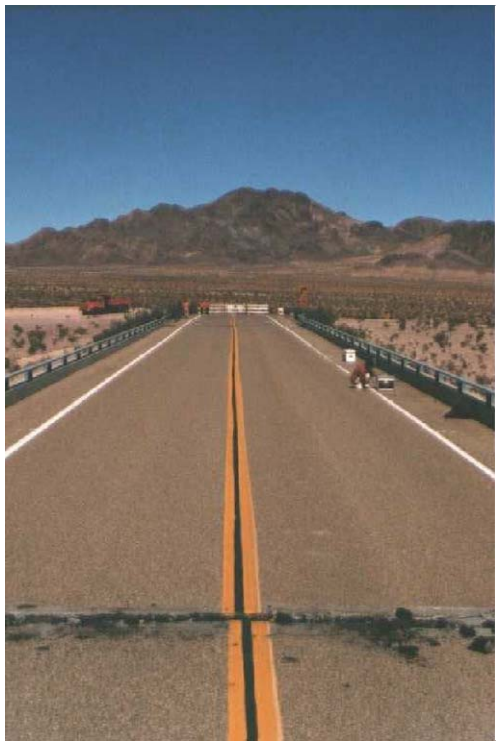

Fig. 8. A view from the south approach to the bridge after the earthquake.

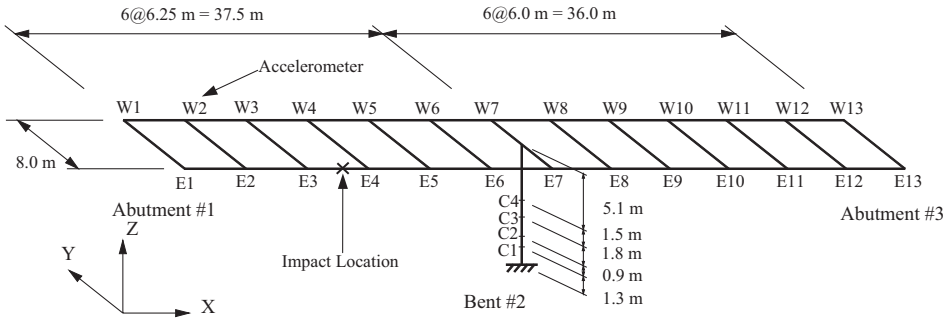

Fig. 9. Locations of accelerometers on the bridge.

5.2. *Results of field modal tests*

Since four effective parameters were selected, the objective of the field testing was to extract at least four of the lower modes of the structure. In the December 1997 test, the lower five modes were selected. These modes were earlier identified in an accompanying FE model of the structure. The selected modes can be described as follows: (1) the first bending mode of the deck about the Y-axis; (2) the first lateral bending mode of the deck about the Z-axis; (3) the second bending

mode of the deck about the Y-axis; (4) the first torsional mode of the deck about the X-axis; and (5) the second lateral bending mode of the deck about the Z-axis. The frequencies associated with these modes are listed in Table 8. In the other three tests, the lower four modes were selected from the measurements. The first lateral bending mode about the Z-axis was not identified in the 1998 and 1999 tests. Note that identified mode shapes are provided in Fig. 10 for the September 1997 test.

Table 8
Measured resonant frequencies

Mode	Dec. 1997	Sep. 1998	Sep. 1999	Oct. 1999
1 (1st bending in Z dir.)	3.099	3.374	3.184	2.627
2 (1st bending in Y dir.)	3.219	—	—	—
3 (2nd bending in Z dir.)	4.426	4.839	4.770	3.891
4 (1st torsion)	6.781	6.740	6.683	5.400
5 (2nd bending in Y dir.)	8.307	8.605	8.550	6.701

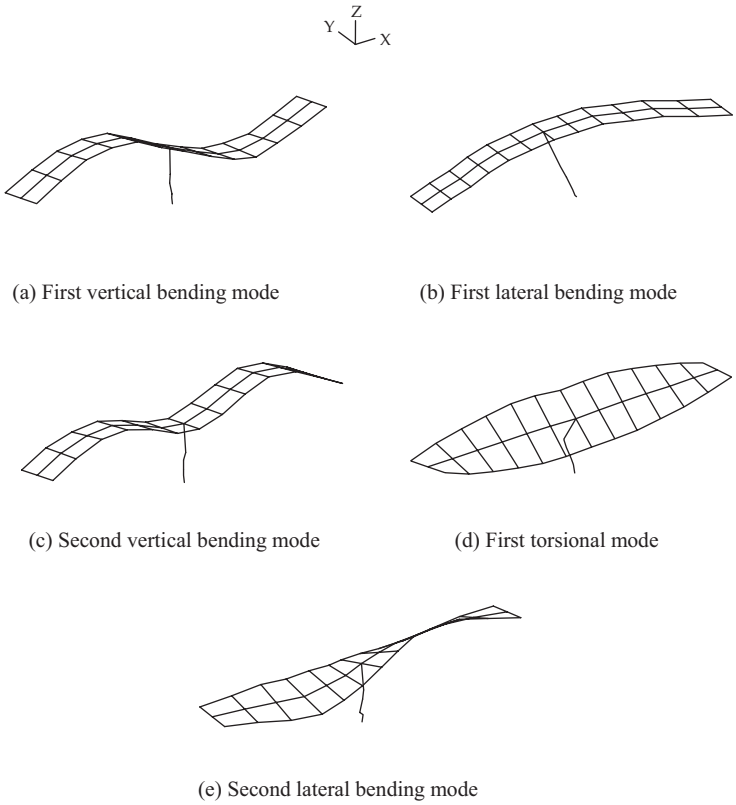

(a) First vertical bending mode

(b) First lateral bending mode

(c) Second vertical bending mode

(d) First torsional mode

(e) Second lateral bending mode

Fig. 10. Extracted modes from the 1997 field measurements.

6. Identification of mass and stiffness changes

The identification procedure consisted of the following three steps: (1) assume an initial set of parameter values for the FE model, (2) generate stiffness and mass sensitivities using the FE model, and (3) update the material properties of the FE model using the procedure outlined in the preceding section. In the first step of the SI process, each member of the FE model shown in Fig. 3 was assigned to one of three groups: Group 1, which included all elements in the deck; Group 2, which included the column and footing of Bent #2; and Group 3, which included the abutment–soil systems. Note that even though the elastic properties for each group are constant, the geometric properties for various sections in that group may vary. For example, the deck is comprised of sections with six different values for the second moment of area. Initial material properties for the FE model were generated as follows: (1) reinforced concrete was assumed to have a mass density of $\rho = 3190\,\mathrm{kg/m^3}$, Poisson ratio of $\nu = 0.15$, and elastic modulus of 27.6 GPa; and (2) the soil was assumed to have a modulus of subgrade reaction of $k_s = 342.7\,\mathrm{MN/m}$ (medium dense sand). The initial material properties of the 1999 October FE model were taken to be those identified properties of the 3rd test. Note that in order to define the characteristics of the system to accommodate the extreme climatic conditions, the systems identification procedures accounted for both changes in mass and stiffness during the period of interest. Note also that four unknowns are to be identified for the FE model for each test. The mass and stiffness properties of the bridge were identified using the seven-step algorithm presented in the previous section. The convergence of the system is shown in Tables 9–12. Note that after 10 iterations the maximum difference between the frequency of the updated FE model and the real structure is less than 2% for the 1997 structure and less than 1% for the rest of structures.

7. Discussion of results

The identified properties of the structure are listed in Table 13 and the weather and temperature logs are presented in Table 14. In the tables, fluctuation in mass was observed due to weather conditions. The mass of the deck and column was as high as $2398\,\mathrm{kg/m^3}$ in rainy and wet weather condition during the 1997 test and as low as $1995\,\mathrm{kg/m^3}$ in sunny and dry weather condition during the 1998 test. During the wet season, the mass of the deck could have increased via moisture absorption in the concrete and/or direct retention of water in the cavity of the box

Table 9
System identification (December 1997)

Mode	Frequency of initial FE model	Updated frequencies (Hz)			Frequency of target structure	Error (%)	
		Iter. 2	Iter. 6	Iter. 10		Initial	Final
1	2.950	3.001	3.043	3.046	3.099	4.8	1.7
2	3.019	3.095	3.280	3.286	3.219	6.2	2.1
3	4.249	4.426	4.500	4.506	4.426	4.0	1.8
4	6.228	6.518	6.733	6.746	6.781	8.2	0.5
5	7.163	7.912	8.152	8.176	8.307	13.8	1.6

Table 10
System identification (September 1998)

Mode	Frequency of initial FE model	Updated frequencies (Hz)			Frequency of target structure	Error (%)	
		Iter. 2	Iter. 6	Iter. 10		Initial	Final
1	2.950	3.300	3.354	3.352	3.374	12.6	0.7
2	4.249	4.744	4.880	4.885	4.839	12.2	1.0
3	6.228	6.453	6.710	6.742	6.740	7.6	0.0
4	7.163	8.529	8.585	8.576	8.605	16.8	0.3

Table 11
System identification (September 1999)

Mode	Frequency of initial FE model	Updated frequencies (Hz)			Frequency of target structure	Error (%)	
		Iter. 2	Iter. 6	Iter. 10		Initial	Final
1	2.950	3.120	3.202	3.201	3.182	7.3	0.6
2	4.249	4.514	4.723	4.730	4.770	10.9	0.8
3	6.228	6.217	6.621	6.674	6.683	6.8	0.1
4	7.163	8.390	8.577	8.575	8.550	16.2	0.3

Table 12
System identification (October 1999)

Mode	Frequency of initial FE model	Updated frequencies (Hz)			Frequency of target structure	Error (%)	
		Iter. 2	Iter. 6	Iter. 10		Initial	Final
1	3.201	2.632	2.644	2.642	2.627	21.8	0.6
2	4.730	3.827	3.862	3.857	3.891	21.6	0.9
3	6.674	5.339	5.417	5.408	5.400	23.6	0.2
4	8.575	6.597	6.728	6.704	6.701	28.0	0.1

Table 13
Identified effective properties of the structure

Group		22 Dec. 1997	26 Sep. 1998	22 Sep. 1999	18 Oct. 1999
1	E (GPa)	21.7	23.4	21.7	14.8
	ρ (kg/m^3)	2398	1995	2056	2056
2	E (GPa)	17.4	10.0	9.9	8.1
	ρ (kg/m^3)	2398	1995	2056	2056
3	k (MN/m)	540	334	437	210

girder. Although we have no quantitative data to support this hypothesis, we believe that this weather difference caused the increase in the measured frequencies between the 1997 and 1998 structures. In the measured frequency data presented in Table 8, the measured frequencies of all modes, except the first torsional mode of the 1998 structures, increased compared with those of the 1997 structure. For example, the first bending mode in the Z direction increased by 8.9% (3.374 Hz) in 1998 from 3.099 Hz in 1997. This caused the anomalous stiffness increase in the deck of 1998 structure from 1997 structure. If the mass of the structure were not changed, the frequency of the structure should decrease when damage accumulates in the structure. Note that in general damage is defined by reduction in the stiffness of structural members, however, the local increase of mass due to the accumulation of water in the structure also could indicate damage. Also, as seen in Fig. 12, we believe that the abutment–soil system was more significantly affected by this weather and humidity difference.

A comparison of the identified stiffnesses for 2-year period is provided graphically in Figs. 11 and 12. In the figures, except the stiffness of the 1997 structures, the stiffness of the deck and column decreased reflecting the effect of time on the stiffness of the structural members. The effective reduction in stiffnesses of the deck, column, and abutments were, respectively, 32%, 53%, and 61% from 1997 to 1999. Especially, after the earthquake, the effective reduction in stiffnesses of the deck, columns, and abutments were, respectively, 32%, 18%, and 52%. In Table 15, the stiffness reductions in the bridge are further quantified. The method utilized here, updating of the FE model, agrees well with stiffness reduction calculated directly from changes in eigensensitivity [10].

Table 14
Weather and temperature logs

	22 Dec. 1997	26 Sep. 1998	22 Sep. 1999	18 Oct. 1999
Weather	Cold, rainy	Sunny, dry	Cloudy	Sunny, dry
Temperature (°C)	4–10	16–21	23–24	16–17

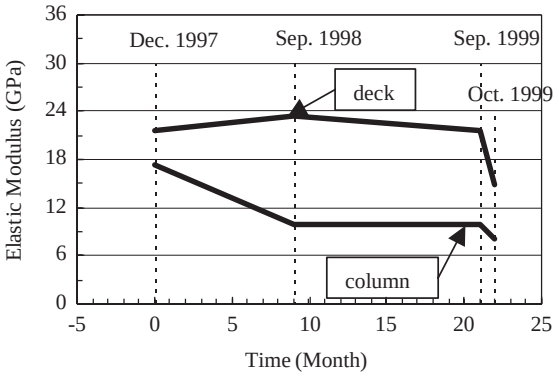

Fig. 11. Changes in elastic modulus of the deck and column.

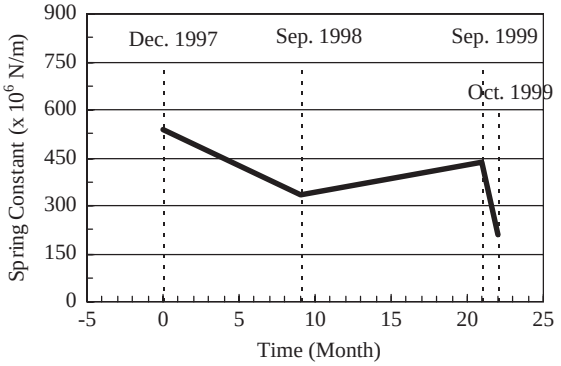

Fig. 12. Changes in spring constant of abutment–soil system.

Table 15
Summary of stiffness changes for September 1999–October 1999

Component	Method	
	SI of baseline structure	Direct utilization of measured frequencies
Deck stiffness	32% decrease	32% decrease
Deck mass	Assumed to be not changed	Assumed to be not changed
Column stiffness	18% decrease	22% decrease
Abutments	52% decrease	56% decrease

8. Summary and conclusions

The objective of this paper is to quantitatively evaluate the rate of possible structural property changes of the reinforced concrete box-girder bridge structure. A total of four field dynamic testing has been conducted from 1997 to 1999 and each time the effective stiffness of the deck, column, and abutments of the bridge was estimated using the system identification method presented in this paper. It was found that the effective reduction in stiffnesses of the deck, column, and abutments were, respectively, 32%, 53%, and 61%. Most of these stiffness reductions can be attributed to the damage by the earthquake that caused the effective reduction in stiffnesses of the deck, columns, and abutments, respectively, 32%, 18%, and 52%. These quantitative estimates of the damage are consistent with the visual damage sustained by the structure directly after the earthquake.

On the basis of the methodology proposed and the results obtained in this study, several conclusions are presented. First, high quality experimental data, which correlates highly with FE predictions, can be obtained for the class of civil engineering structures discussed in this study. Second, field modal data can be collected efficiently (within 2–3 h for a single test) and in a timely manner (within 2 days after an earthquake) for this common class of structures. Third, combining state-of-the-art identification schemes such as model updating with actual field measurements, the changes in structural properties for major structural components in real structures can be

quantified. Fourth, environmental conditions, such as the extreme differences in the atmospheric moisture conditions during the wet winter months and the dry summer months in the region, may significantly affect the accuracy of the SI. Finally, from knowledge of changes in stiffness properties of components, various quantitative measures of damage [14] can be formulated; these measures can then be correlated with magnitudes of the hazard at the location of the structure. In other words, the approach suggested in this study may lead to a methodology that can estimate and monitor structural damage quantitatively and periodically for specific structures.

Acknowledgements

Funding for this study was sponsored by State of California Department of Transportation (CALTRANS) under contract number 59A0022.

References

[1] C.R. Farrar, G.H. James, System identification from ambient vibration measurements on a bridge, *Journal of Sound and Vibration* 205 (1997) 1–18.
[2] J.L. Beck, M.W. Vanik, D.C. Polidori, B.S. May, Structural health monitoring using ambient vibrations, *Proceedings of the Structural Engineers World Congress*, Reston, Virginia, Paper T118-3, 1998.
[3] C.R. Farrar, D.A. Jauregui, Comparative study of damage identification algorithms applied to a bridge: I. experiment, *Journal of Smart Materials and Structures* 7–5 (1998) 704–719.
[4] C.R. Farrar, D.A. Jauregui, Comparative study of damage identification algorithms applied to a bridge: II. Numerical study, *Journal of Smart Materials and Structures* 7–5 (1998) 720–731.
[5] S.W. Doebling, C.R. Farrar, M.B. Prime, D.W. Shevitz, Damage identification and health monitoring of structural and mechanical systems from changes in their vibration characteristics: a literature review, Technical Report LA-13070-MS, Los Alamos National Laboratory, Los Alamos, NM, 1996.
[6] D.F. Mazurek, J.T. DeWolf, Experimental study of bridge monitoring technique, *Journal of Structural Engineering* 116–9 (1990) 2532–2549.
[7] M.W. Vanik, J.L. Beck, A Bayesian probabilistic approach to structural health monitoring, *Proceedings of 16th International Modal Analysis Conference*, Santa Barbara, California, 1998, pp. 342–348.
[8] S. Park, N. Stubbs, R. Bolton, S. Choi, C. Sikorsky, Field verification of the damage index method in a concrete box-girder bridge via visual inspection, *Computer-Aided Civil and Infrastructure Engineering* 16 (2001) 58–70.
[9] N. Stubbs, J.T. Kim, Damage localization in structures without baseline modal parameters, *American Institute of Aeronautics and Astronautics Journal* 34–8 (1996) 1644–1649.
[10] N. Stubbs, R. Osegueda, Global non-destructive damage evaluation in solids, *International Journal of Analytical and Experimental Modal Analysis* 5–2 (1990) 67–79.
[11] ABAQUS Version 5.4 User's Manual, Hibbitt, Karlsson & Sorensen Inc, Providence, RI, 1994.
[12] D.J. Ewins, *Modal Testing*: *Theory and Practice*, Research Studies Press, Hertfordshire, 1986.
[13] R.W. Bolton, N. Stubbs, C. Sikorsky, S. Park, S. Choi, D. Nam, Measurement of structural parameters for modal based non-destructive damage detection of bridges, ICOSSAR 2000, 2000.
[14] L.M. Kachanov, *Introduction to Continuum Damage Mechanics*, Kluwer Academic Publishers, Dordrecht, Netherlands, 1986.